

# Dark Matter Signals on a Laser Interferometer

Satoshi Tsuchida\*

*Department of Physics, Osaka City University, Osaka, Osaka, 558-8585, Japan*

Nobuyuki Kanda and Yousuke Itoh

*Department of Physics, Osaka City University, Osaka, Osaka, 558-8585, Japan,  
Nambu Yoichiro Institute of Theoretical and Experimental Physics (NITEP),  
Osaka City University, Osaka, Osaka, 558-8585, Japan*

Masaki Mori

*Department of Physical Science, Ritsumeikan University, Kusatsu, Shiga, 525-8577, Japan*  
(Dated: September 10, 2019)

WIMPs are promising dark matter candidates. A WIMP occasionally collides with a mirror equipped with interferometric gravitational wave detectors such as LIGO, Virgo, KAGRA and Einstein Telescope (ET). When WIMPs collide with a mirror of an interferometer, we expect that characteristic motions of the pendulum and mirror are excited, and those signals could be extracted by highly sophisticated sensors developed for gravitational wave detection. We analyze the motions of the pendulum and mirror, and estimate the detectability of these motions. For the “Thin-ET” detector, the signal to noise ratio may be  $1.7 \left( \frac{m_{\text{DM}}}{100 \text{ GeV}} \right)$ , where  $m_{\text{DM}}$  is the mass of a WIMP. We may set a more strict upper limit on the cross section between a WIMP and a nucleon than the limits obtained by other experiments so far when  $m_{\text{DM}}$  is approximately lower than 0.2 GeV. We find an order of magnitude improvement in the upper limit around  $m_{\text{DM}} = 0.2 \text{ GeV}$ .

PACS numbers: 95.35.+d, 04.30.-w, 04.80.Nn

## I. INTRODUCTION

The first direct detection of a gravitational wave (GW) event was achieved by LIGO (Laser Interferometer Gravitational-Wave Observatory) in 2015 [1]. To date, ten binary black hole mergers [1–6] and one binary neutron star signal [7] were detected in the first and second LIGO/Virgo observing runs (O1, O2). LIGO and Virgo started the third observing run (O3) in April 2019. KAGRA, the first cryogenic underground GW observatory, is now under construction in Japan [8–11], and it is planned to join the O3. In addition, the third generation GW detectors such as Einstein Telescope (ET) [12] and Cosmic Explorer [13] are being proposed. As the sensitivities of the current generation GW detectors are so high, these detectors can be sensitive to not only GWs but also external agents. Namely, GW detectors could extract signals caused by dark matter particles colliding with a mirror equipped with interferometers.

Candidates for dark matter may be categorized into two types. One is macroscopic matter, such as MACHOs (Massive Compact Halo Objects), whereas the other is microscopic matter, such as WIMPs (Weakly Interacting Massive Particles). WIMPs are believed to be good candidates for dark matter to explain the structure of the present Universe, and have extensive allowed mass range of about 0.1 GeV to 10 TeV. Methods explored so far to hunt for WIMPs include collider searches, indirect detections, and direct detections: for details, see e.g. Refs. [14, 15]. To prove the existence of WIMPs, the direct detections, where one observes possible nuclear recoils after WIMP–nucleon elastic scattering, would be the most suitable method. The cross section between a WIMP and a nucleon is expected to be extremely small. So far, a couple of research groups have reported positive signals [16–18], but the results are still controversial and it seems still premature to claim the existence of a WIMP.

We propose a search method for WIMP signals using laser interferometric gravitational wave detectors. Possible dark matter signals on laser interferometers have been investigated in several works [19–21]. However, calculations of the signals caused by direct interaction between a WIMP and nucleons in the mirror of interferometers have not been considered in the literature yet.

---

\*Satoshi Tsuchida: tsuchida@gwv.hep.osaka-cu.ac.jp

In this paper, we solve equations of motion for the behavior of the pendulum and mirror induced by a WIMP collision with the mirror, and obtain the characteristic amplitude spectrum. Then, we derive the signal to noise ratio by comparing the signals to the design sensitivity of each detector, and set an upper limit on the cross section between a WIMP and a nucleon.

## II. DARK MATTER FLUX AND EVENT RATE

The dark matter flux,  $\Phi_{\text{DM}}$ , around the Earth is given as follows [22]:

$$\begin{aligned}\Phi_{\text{DM}} &= n_{\text{DM}} \times \langle v \rangle = \frac{\rho_{\text{DM}}}{m_{\text{DM}}} \langle v \rangle \\ &\cong 6.6 \times 10^4 \text{ cm}^{-2} \text{ s}^{-1} \left( \frac{\rho_{\text{DM}}}{0.3 \text{ GeV/cm}^3} \right) \left( \frac{100 \text{ GeV}}{m_{\text{DM}}} \right) \left( \frac{\langle v \rangle}{220 \text{ km/s}} \right),\end{aligned}\quad (1)$$

where  $n_{\text{DM}}$  is the number density of WIMPs,  $\langle v \rangle$  is the mean velocity of WIMPs,  $\rho_{\text{DM}}$  is the local dark matter density, and  $m_{\text{DM}}$  is the mass of WIMPs. Using this flux, we can estimate the event rate,  $R$ , of WIMP collisions with nucleons near the Earth as follows:

$$\begin{aligned}R &= \frac{N_{\text{A}}}{A} \Phi_{\text{DM}} \sigma_{\text{WN}}(A) \\ &\cong 0.13 \frac{\text{events}}{\text{kg} \cdot \text{year}} \left( \frac{100 \text{ g/mol}}{A} \right) \left( \frac{\rho_{\text{DM}}}{0.3 \text{ GeV/cm}^3} \right) \left( \frac{100 \text{ GeV}}{m_{\text{DM}}} \right) \left( \frac{\langle v \rangle}{220 \text{ km/s}} \right) \left( \frac{\sigma_{\text{WN}}(A)}{10^{-38} \text{ cm}^2} \right),\end{aligned}\quad (2)$$

where  $N_{\text{A}} = 6.02 \times 10^{23} \text{ mol}^{-1}$  is the Avogadro constant,  $A$  is the molar mass of the target nucleus, and  $\sigma_{\text{WN}}(A)$  is the cross section between a WIMP and a nucleon. The value of cross section may affect on the lifetime of WIMPs, thus the evaluation of the cross section could play a important role to elucidate the nature of WIMPs.

## III. EXPECTED DARK MATTER SIGNALS

The schematic image for a collision of a WIMP with the mirror is shown in Fig. 1. The parameters  $M_{\text{T}}$ ,  $E$ ,  $\rho$ ,  $\nu$ ,  $a$ , and  $h$  in Fig. 1 are the mass, Young's modulus, matter density, Poisson's ratio, radius, and thickness of the mirror, respectively. The values of these parameters for the detectors are given in Table I. When a WIMP collides with a nucleon in the mirror, we expect that various characteristic motions of the pendulum and mirror occur. In this paper, we consider the induced signals due to (i) pendulum (translation) motion and (ii) elastic oscillation of the mirror. We do not consider other motions such as the rotation of the mirror or violin mode of the pendulum, and so on. Here, we derive the expressions for signals due to (i) and (ii).

(i) *Pendulum (translation) motion*: Firstly, we consider the translation of the mirror, namely motion of the pendulum. The equation of motion for this mode is given by

$$\frac{d^2 z_{\text{Pend}}(t)}{dt^2} + \frac{2\pi f_0}{Q_{\text{P}}} \frac{dz_{\text{Pend}}(t)}{dt} + (2\pi f_0)^2 z_{\text{Pend}}(t) = \frac{F(t)}{M_{\text{T}}}, \quad (3)$$

where  $Q_{\text{P}} \sim 10^7$  is the quality factor,  $f_0 \simeq 1 \text{ Hz}$  is the resonance frequency of the pendulum, and  $F(t)$  is the external force given by a WIMP collision:

$$F(t) = P_{\text{DM}} \delta(t), \quad (4)$$

where  $P_{\text{DM}} = m_{\text{DM}} v_{\text{DM}}$  is the momentum of a WIMP,  $v_{\text{DM}} = 220 \text{ km/s}$  is the typical velocity of WIMPs, and we assume the collision happens at  $t = 0$ . Here, we assume the delta-functional force for  $F(t)$ . When a WIMP that has  $m_{\text{DM}} = 100 \text{ GeV}$  collides with a nucleon in the mirror and scatters elastically, the nucleon will have kinetic energy of about 30 keV. This energy may be higher than the binding energy of intermolecular force in the mirror, so the nucleon would give rise to a “secondary” nucleon. By using the SRIM (The Stopping and Range of Ions in Matter) calculation tool [23], we can show that the secondary nucleon may be stopped within about  $10^{-12} \text{ s}$ , and this time scale is much shorter than the sampling time of gravitational wave data acquisition systems. Thus, we can ignore the effect of the secondary nucleon, and we can approximately describe the collision using a delta function as in Eq. (4).

The solution of the equation of motion (3) is obtained as in a damped sinusoidal waveform:

$$z_{\text{Pend}}(t) = \frac{P_{\text{DM}}}{2\pi M_{\text{T}} f_0 \sqrt{1 - \frac{1}{4Q_{\text{P}}^2}}} \exp \left[ -\frac{\pi f_0}{Q_{\text{P}}} t \right] \sin \left( 2\pi f_0 \sqrt{1 - \frac{1}{4Q_{\text{P}}^2}} t \right). \quad (5)$$

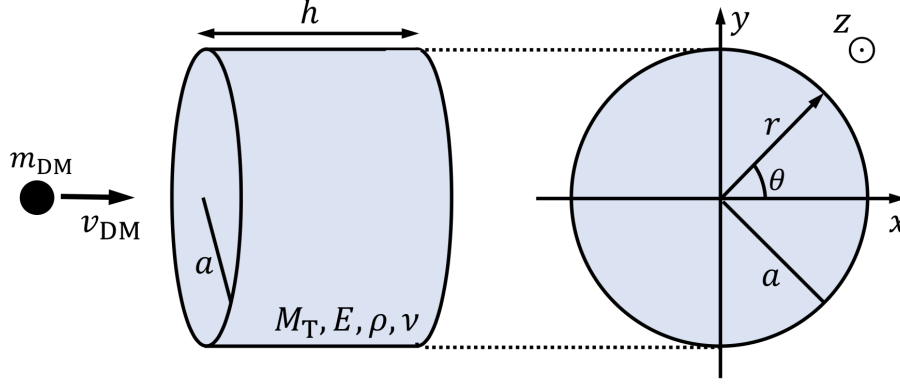


FIG. 1: (Color Online). The schematic image for a collision of a WIMP with the mirror equipped with a laser interferometer.

Using Fourier transformation defined as  $\tilde{z}(f) = \int_{-\infty}^{\infty} z(t)e^{-2\pi ift}dt$ , this solution can be written in the frequency domain as follows:

$$|\tilde{z}_{\text{Pend}}(f)| = \frac{P_{\text{DM}}}{4\pi^2 M_T} \frac{1}{\sqrt{(-f^2 + f_0^2)^2 + \left(\frac{ff_0}{Q_F}\right)^2}}. \quad (6)$$

This expression shows that the signal caused by the motion of the pendulum has a sharp peak at the resonance frequency  $f = f_0$ , and the signal is proportional to  $f^{-2}$  at higher frequencies than  $f_0$ .

(ii) *Elastic oscillation of the mirror*: Secondly, we consider the elastic oscillation of the mirror induced by a WIMP collision with the mirror that has a cylindrical shape. The equation of motion is given by

$$\frac{\partial^2 z_{\text{Elas}}(t, r, \theta)}{\partial t^2} + \frac{2\pi f_e}{Q_M} \frac{\partial z_{\text{Elas}}(t, r, \theta)}{\partial t} + \mathcal{D} (\nabla^2)^2 z_{\text{Elas}}(t, r, \theta) = 0, \quad (7)$$

where  $\mathcal{D} = \frac{Eh^2}{12\rho(1-\nu^2)}$  is the flexural rigidity,  $Q_M \sim 10^7$  is the quality factor of the mirror,  $f_e$  is the eigen frequency of the elastic oscillation, and  $\nabla^2$  is the two dimensional Laplacian. The solution of Eq. (7) is given by

$$z_{\text{Elas}}(t, r, \theta) = \sum_{m=0}^{\infty} \cos(m\theta) \sum_{n=0}^{\infty} K_{mn} R_{mn}(r) \exp\left[-\frac{\pi f_{mn}}{Q_M} t\right] \sin\left(2\pi f_{mn} \sqrt{1 - \frac{1}{4Q_M^2}} t\right), \quad (8)$$

where  $m$  corresponds to the number of nodal diameters,  $n$  is the number of nodal circles,  $f_{mn}$  denotes the eigen frequency for each mode,  $K_{mn}$  is a numerical constant depending on initial conditions, and  $R_{mn}(r)$  is a function of  $r$ , which will be given below.

As for the boundary condition, we assume that the mirror is a completely free cylinder, since the mirror is not clamped. In this situation, at the edge of the circle of the cylinder,  $r = a$ , bending moment  $M_r(r = a)$  and shearing

TABLE I: Characteristic quantities of the mirrors for the interferometers.

	The Name of Laser Interferometers		
	KAGRA	LIGO, Virgo	Einstein Telescope
Material	Sapphire	Fused Silica	Fused Silica
Molar mass, $A$ [g/mol]	101.96	60.08	60.08
Mirror Mass, $M_T$ [kg]	23	40	200
Density, $\rho$ [g/cm <sup>3</sup> ]	4.00	2.20	2.20
Radius, $a$ [cm]	11	17.5	31
Thickness, $h$ [cm]	15	20	30
Young's modulus, $E$ [GPa]	400	72.6	72.6
Poisson's ratio, $\nu$	0.3	0.16	0.16

force  $V_r(r=a)$  should be zero, that is, these satisfy the following conditions:

$$\begin{aligned} M_r(r)|_{r=a} &= \left[ \frac{\partial^2 z_{\text{Elas}}}{\partial r^2} + \nu \left( \frac{1}{r} \frac{\partial z_{\text{Elas}}}{\partial r} + \frac{1}{r^2} \frac{\partial^2 z_{\text{Elas}}}{\partial \theta^2} \right) \right] \bigg|_{r=a} = 0, \\ V_r(r)|_{r=a} &= \left[ \frac{\partial}{\partial r} (\nabla^2 z_{\text{Elas}}) + \frac{1-\nu}{r} \frac{\partial}{\partial r} \left( \frac{1}{r} \frac{\partial z_{\text{Elas}}}{\partial \theta} \right) \right] \bigg|_{r=a} = 0. \end{aligned} \quad (9)$$

These boundary conditions lead to the eigenvalue equation:

$$\frac{\lambda_{mn}^2 J_m(\lambda_{mn}) + (1-\nu) [\lambda_{mn} J'_m(\lambda_{mn}) - m^2 J_m(\lambda_{mn})]}{\lambda_{mn}^2 I_m(\lambda_{mn}) - (1-\nu) [\lambda_{mn} I'_m(\lambda_{mn}) - m^2 I_m(\lambda_{mn})]} = \frac{\lambda_{mn}^3 J'_m(\lambda_{mn}) + (1-\nu) m^2 [\lambda_{mn} J'_m(\lambda_{mn}) - J_m(\lambda_{mn})]}{\lambda_{mn}^3 I'_m(\lambda_{mn}) - (1-\nu) m^2 [\lambda_{mn} I'_m(\lambda_{mn}) - I_m(\lambda_{mn})]}, \quad (10)$$

where  $\lambda_{mn} = \Omega_{mn} a$ ,  $\Omega_{mn}^4 = \frac{(2\pi f_{mn})^2}{D}$ ,  $J_m(\lambda)$  is a Bessel function,  $I_m(\lambda)$  is a modified Bessel function,  $J'_m(\lambda) = \frac{\partial J_m(\lambda)}{\partial \lambda}$ , and  $I'_m(\lambda) = \frac{\partial I_m(\lambda)}{\partial \lambda}$ . From these relations, we obtain the eigen frequency for each mode, and these frequencies are listed in Table II. As can be expected, the eigen frequency of each mode is smaller for a softer and thinner mirror. The material of the mirrors equipped with the KAGRA is sapphire, which is harder than fused silica that constitutes the mirrors of LIGO and Virgo, so the eigen frequency of each mode for KAGRA is higher than that for the other mirrors. On the other hand, the mirrors for ET are relatively thinner than the mirrors for KAGRA, LIGO and Virgo, thus the mirrors for ET have a lower eigen frequency for each mode.

Then, we derive the displacement of the mirror and function  $R_{mn}(r)$  by using Eqs. (9) and (10), so the solution of Eq. (7) is written as

$$\begin{aligned} z_{\text{Elas}}(t, r, \theta) &= \sum_{m=0}^{\infty} \cos(m\theta) \sum_{n=0}^{\infty} K_{mn} R_{mn}(r) \exp \left[ -\frac{\pi f_{mn}}{Q_M} t \right] \sin \left( 2\pi f_{mn} \sqrt{1 - \frac{1}{4Q_M^2}} t \right) \\ \text{with } R_{mn}(r) &= \left[ J_m(\Omega_{mn} r) + \frac{\lambda_{mn}^3 J'_m(\lambda_{mn}) + (1-\nu) m^2 [\lambda_{mn} J'_m(\lambda_{mn}) - J_m(\lambda_{mn})]}{\lambda_{mn}^3 I'_m(\lambda_{mn}) - (1-\nu) m^2 [\lambda_{mn} I'_m(\lambda_{mn}) - I_m(\lambda_{mn})]} I_m(\Omega_{mn} r) \right]. \end{aligned} \quad (11)$$

Using Fourier transformation, we obtain the displacement in the frequency domain as

$$|\tilde{z}_{\text{Elas}}(f, r, \theta)| \simeq \frac{1}{2\pi} \sqrt{1 - \frac{1}{4Q_M^2}} \sum_{m=0}^{\infty} \cos(m\theta) \sum_{n=0}^{\infty} K_{mn} f_{mn} R_{mn}(r) \frac{1}{\sqrt{(-f^2 + f_{mn}^2)^2 + \left( \frac{f f_{mn}}{Q_M} \right)^2}}, \quad (12)$$

thus, the signal caused by elastic oscillation also has sharp peaks at the resonance frequencies  $f = f_{mn}$ . To calculate  $K_{mn}$ , we consider the momentum conservation law that is given by

$$P_{\text{DM}} \delta(\mathbf{r} - \mathbf{r}_0) = 2\pi \rho h \sum_{m=0}^{\infty} \cos(m\theta) \sum_{n=0}^{\infty} K_{mn} f_{mn} R_{mn}(r), \quad (13)$$

where  $\mathbf{r}_0 = (r_0, \theta_0)$  means the collision point of the WIMP on the mirror. We multiply  $R_{pq}(r) \cos(p\theta)$  to the both sides, and integrate over the entire region of the mirror surface, then we obtain

$$P_{\text{DM}} R_{mn}(r_0) \cos(m\theta_0) = 2\pi \rho h K_{mn} f_{mn} \int_0^a R_{mn}^2(r) r dr \int_0^{2\pi} \cos^2(m\theta) d\theta. \quad (14)$$

TABLE II: The value of eigen frequency in unit of  $\times 10^4$  [Hz] for each  $m$  and  $n$  for KAGRA (LIGO, Virgo) [ET].

	$m=0$	$m=1$	$m=2$	$m=3$	$m=4$	$m=5$
$n=0$	—	—	3.20 (1.01) [0.481]	7.43 (2.31) [1.10]	13.0 (4.03) [1.93]	20.0 (6.15) [2.94]
$n=1$	5.38 (1.51) [0.724]	12.2 (3.54) [1.69]	21.1 (6.17) [2.95]	31.6 (9.33) [4.46]	43.9 (13.0) [6.20]	57.8 (17.1) [8.17]
$n=2$	23.0 (6.66) [3.18]	35.7 (10.4) [4.97]	50.4 (14.7) [7.04]	66.8 (19.6) [9.36]	85.0 (25.0) [11.9]	105 (30.8) [14.7]
$n=3$	52.4 (15.3) [7.30]	71.0 (20.7) [9.91]	91.5 (26.8) [12.8]	114 (33.3) [15.9]	138 (40.4) [19.3]	164 (48.0) [22.9]
$n=4$	93.6 (27.3) [13.1]	118 (34.5) [16.5]	145 (42.2) [20.2]	173 (50.5) [24.1]	203 (59.3) [28.3]	234 (68.6) [32.8]
$n=5$	147 (42.8) [20.5]	177 (51.7) [24.7]	209 (61.2) [29.2]	243 (71.2) [34.0]	279 (81.7) [39.0]	317 (92.7) [44.3]

We note that the modes that contribute to the displacement at the center of the circle of the mirror should play a key role to evaluate the effects of the signals caused by a WIMP collision, since laser beams used for measuring the differential displacement of the arm length irradiate the center of the circle of the mirror. Thus, hereafter, we only consider the elastic oscillations at the center of the circle that correspond to  $m = 0$  modes.

We derive the numerical factor  $K_{0n}$  for each  $n$  mode as follows:

$$K_{0n}(r_0) = \frac{P_{\text{DM}} R_{0n}(r_0)}{4\pi^2 \rho h f_{0n} \int_0^a R_{0n}^2(r) r dr}. \quad (15)$$

Using  $K_{0n}$ , we obtain the magnitude of the displacement at  $f = f_{0n}$  and  $r = 0$  for each  $n$  mode and  $r_0$  as follows:

$$|\tilde{z}_{\text{Elas}}(f = f_{0n}, r = 0)| = \left| \frac{1}{2\pi} \sqrt{1 - \frac{1}{4Q_M^2}} K_{0n}(r_0) R_{0n}(r = 0) Q_M \frac{1}{f_{0n}} \right|. \quad (16)$$

The values of them are summarized in Table III with  $m_{\text{DM}} = 100$  GeV. When a WIMP collides with the mirror at the center of the circle ( $r_0 = 0$ ), the displacement  $|\tilde{z}_{\text{Elas}}(f = f_{0n}, r = 0)|$  attains the maximum for each  $n$  mode.

#### IV. LIMIT ON THE CROSS SECTION BETWEEN A WIMP AND A NUCLEON

Here, we calculate the signal to noise ratio (SNR)  $\varrho$ , and estimate the upper limit on the cross section between a WIMP and a nucleon  $\sigma_{\text{WN}}$ . To calculate the SNR, we introduce the characteristic amplitude spectrum  $\sqrt{S_a(f)}$  that is defined by

$$\sqrt{S_a(f)} = \sqrt{4f \frac{|\tilde{z}(f)|^2}{L^2}}, \quad (17)$$

where the square modulus of the amplitude  $|\tilde{z}(f)|^2$  is given by  $|\tilde{z}(f)|^2 = |\tilde{z}_{\text{Pend}}(f)|^2 + |\tilde{z}_{\text{Elas}}(f)|^2$ , and  $L$  is the arm length of an interferometer. Using the spectrum  $\sqrt{S_a(f)}$ , the SNR is given by

$$\varrho^2 = \int_{f_{\min}}^{f_{\max}} \frac{S_a(f)}{S_n(f)} \frac{df}{f}, \quad (18)$$

where  $S_n(f)$  is the one-sided power spectral density of the detector in consideration,  $f_{\min}$  and  $f_{\max}$  are the minimum and the maximum frequencies of the design sensitivity curves for the detectors given in Refs. [25, 26]. As mentioned above, the signal spectrum  $S_a(f)$  has sharp peaks at the eigen frequencies and small values for other frequency regions, so the contributions of the peaks predominantly increase the SNR. However, the most of eigen frequencies for KAGRA, LIGO, Virgo and ET are outside of the sensitivity curves for the detectors, thus the SNR cannot attain enough values to detect these signals.

TABLE III: The magnitude of the displacement  $|\tilde{z}_{\text{Elas}}(f = f_{0n}, r = 0)|$  ( $\times 10^{-26}$ ) for KAGRA (LIGO, Virgo) [ET] with  $m_{\text{DM}} = 100$  GeV.

	The collision point of the WIMP on the mirror, $r_0$					
	0.0a	0.1a	0.2a	0.3a	0.4a	0.5a
$n = 1$	60.8 (404) [376]	59.2 (394) [366]	54.4 (363) [337]	46.8 (312) [290]	36.7 (246) [229]	24.6 (166) [155]
$n = 2$	8.19 (52.4) [48.8]	7.42 (47.6) [44.2]	5.35 (34.4) [32.0]	2.54 (16.5) [15.4]	0.23 (1.19) [1.11]	2.25 (14.2) [13.2]
$n = 3$	2.34 (14.9) [13.8]	1.86 (11.8) [11.0]	0.70 (4.44) [4.13]	0.44 (2.79) [2.60]	0.94 (5.98) [5.56]	0.65 (4.15) [3.85]
$n = 4$	0.98 (6.19) [5.76]	0.63 (4.00) [3.72]	0.05 (0.31) [0.28]	0.39 (2.49) [2.31]	0.17 (1.09) [1.01]	0.21 (1.33) [1.24]
$n = 5$	0.50 (3.15) [2.93]	0.24 (1.50) [1.39]	0.15 (0.95) [0.88]	0.13 (0.85) [0.79]	0.11 (0.68) [0.63]	0.10 (0.66) [0.61]
	0.6a	0.7a	0.8a	0.9a	1.0a	—
$n = 1$	11.3 (77.4) [72.0]	2.87 (17.3) [16.1]	17.2 (114) [106]	31.4 (211) [197]	45.1 (307) [285]	
$n = 2$	3.04 (19.4) [18.0]	2.50 (16.1) [14.9]	0.88 (5.83) [5.42]	1.35 (8.44) [7.85]	3.72 (23.9) [22.2]	
$n = 3$	0.06 (0.36) [0.34]	0.60 (3.75) [3.49]	0.55 (3.48) [3.23]	0.05 (0.28) [0.26]	0.87 (5.50) [5.11]	
$n = 4$	0.26 (1.65) [1.54]	0.02 (0.14) [0.13]	0.23 (1.43) [1.33]	0.07 (0.43) [0.40]	0.31 (1.98) [1.84]	
$n = 5$	0.09 (0.56) [0.52]	0.09 (0.56) [0.52]	0.07 (0.46) [0.42]	0.06 (0.39) [0.36]	0.14 (0.90) [0.84]	

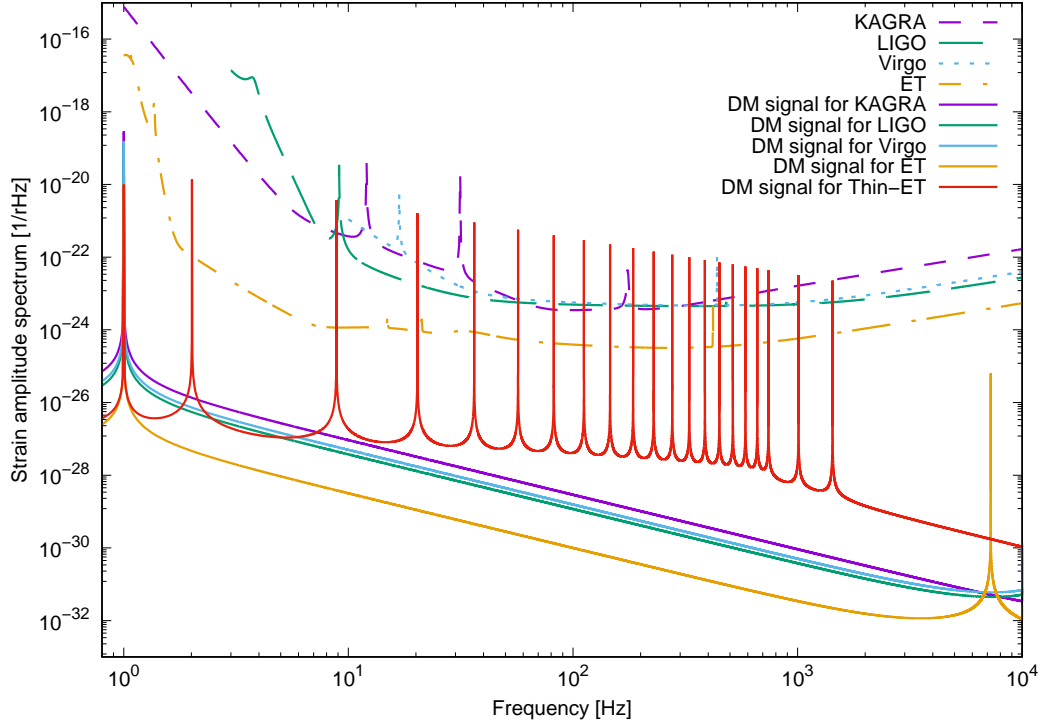


FIG. 2: (Color Online). The characteristic amplitude spectra  $\sqrt{S_a(f)}$  and design sensitivities for the existing or planned interferometers dedicated for gravitational wave observations [25, 26].

Alternatively, we can propose a “Thin-ET” detector to extract the signal caused by a WIMP collision. Mirrors of the Thin-ET detector would have thinner thickness ( $h = 0.5$  cm) and larger radius ( $a = 240$  cm), and the other parameters of the mirrors and the arm length are the same as those of the ET detector. Thus, the sensitivity curve of the Thin-ET detector would be the same as that of ET by using the calculation in Ref. [24]. Since the thin thickness and large radius cylinder has low eigen frequencies, the many sharp peaks can be in the observation frequency band. Thus, we expect that we can obtain a larger SNR for the Thin-ET detector than SNRs for other interferometers. The characteristic amplitude spectra  $\sqrt{S_a(f)}$  and design sensitivities for the existing or planned interferometers dedicated for gravitational wave observations are shown in Fig. 2. This figure indicates that the most of the peak magnitudes at the eigen frequencies for the Thin-ET detector may be higher than the given sensitivity curve, so we expect that the Thin-ET detector has a moderate SNR value. From the above calculation, the SNR is proportional to mass of a WIMP, so we can write the SNR as  $\varrho = \varrho_{\text{fact}} \left( \frac{m_{\text{DM}}}{100 \text{ GeV}} \right)$ , where  $\varrho_{\text{fact}} \simeq 1.7$  for the Thin-ET detector.

Since we know the expected waveform of the dark matter signal considered in this paper, it is most optimal to detect the signal using a detection statistic based on the matched filtering technique, which is widely used in the gravitational wave data analysis community. We declare signal detection if our detection statistic exceeds, say,  $5\sigma$ . If not, we conclude no detection and proceed to set an upper limit on the cross section between a WIMP and a nucleon.

The number of the collision events follows Poisson distribution with the expected number of events  $\lambda$  given by  $\lambda \equiv \epsilon M_T R T_{\text{obs}}$  where  $\epsilon$  is the detection efficiency and  $T_{\text{obs}}$  is the observation time. The detection efficiency may be calculated based on the detection threshold on our detection statistic ( $5\sigma$ ), the expected signal to noise ratio given by Eq. (18), and statistical property of detector noise. We assume that noise of a laser interferometric gravitational wave detector follows stationary Gaussian distribution, which is a good approximation to the first order. The upper limit on the event rate at a 90% confidence level,  $R_{90}$ , may then be calculated using

$$R_{90} = \frac{2.303}{\epsilon M_T T_{\text{obs}}}. \quad (19)$$

Using Eq. (19), we obtain the upper limit on the cross section  $\sigma_{\text{WN}}$  as follows:

$$\sigma_{\text{WN}} \simeq \frac{8.9}{\epsilon} \times 10^{-40} \text{ cm}^2 \left( \frac{200 \text{ kg}}{M_T} \right) \left( \frac{1 \text{ year}}{T_{\text{obs}}} \right) \left( \frac{A}{100 \text{ g/mol}} \right) \left( \frac{m_{\text{DM}}}{100 \text{ GeV}} \right) \left( \frac{240 \text{ cm}}{a} \right) \left( \frac{a + h}{240.5 \text{ cm}} \right), \quad (20)$$

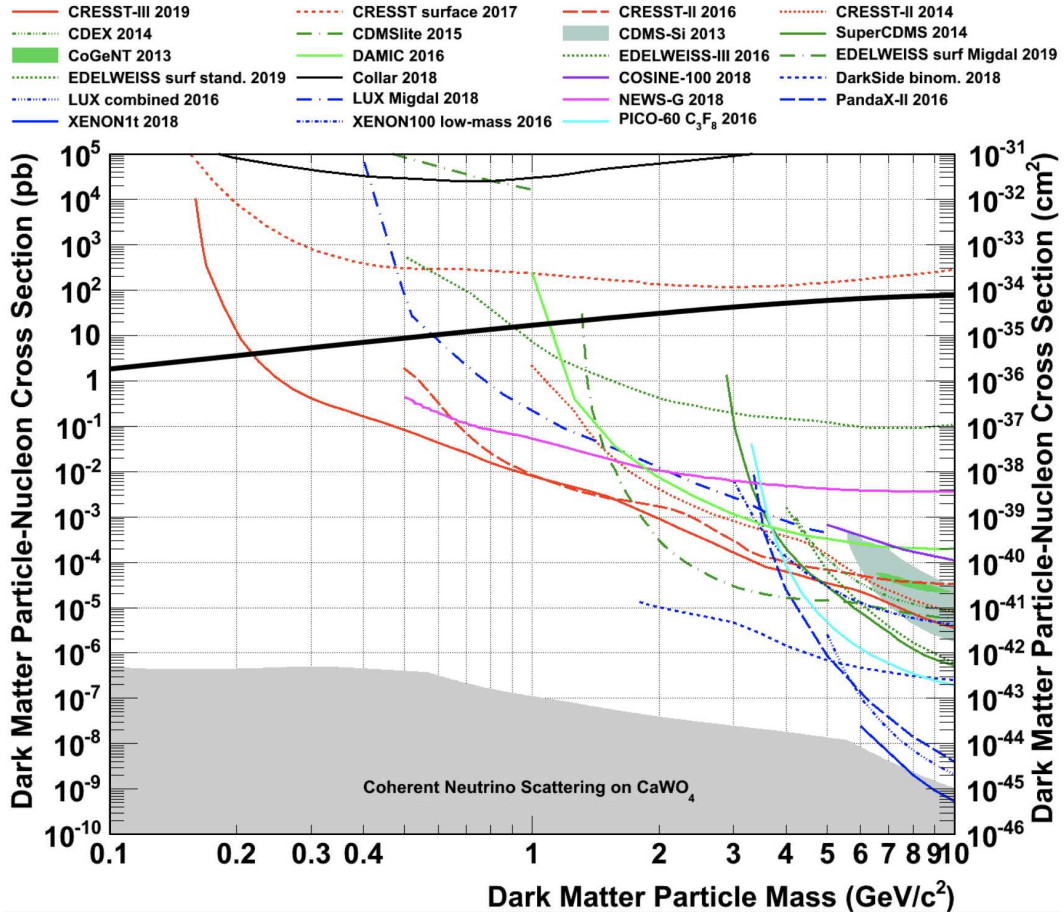


FIG. 3: (Color Online). Upper limits on the cross section  $\sigma_{\text{WN}}$  obtained by our calculation for “Thin-ET” detector (thick solid black line) superimposed on Fig. 7 in Ref. [27]. Detailed discussions for other experimental results obtained so far are given in Refs. [28–47].

where the local dark matter density and the mean velocity of WIMPs are fixed at  $\rho_{\text{DM}} = 0.3 \text{ GeV/cm}^3$  and  $\langle v \rangle = 220 \text{ km/s}$ , respectively. The last two factors in Eq. (20) means the ratio between the surface area of two bottom faces and the total surface area of the mirror. Our possible upper limit on the cross section as a function of the WIMP mass along with those by other experiments are shown in Fig. 3. This figure implies that, in the low WIMP mass region ( $\lesssim 0.2 \text{ GeV}$ ), we could set more strict upper limits on the cross section than the limits obtained so far. When the mass of the WIMP is just a little smaller than  $0.2 \text{ GeV}$ , the upper limit would be improved roughly by an order of magnitude.

We note that we should consider the effects of instrumental noises and have to distinguish target signals from these noises when we analyze real data obtained by interferometric gravitational wave detectors. Detailed discussions and estimations including such instrumental noises and other possible motions of the pendulum and mirror would be considered in future works.

## V. CONCLUSION

When dark matter particles, such as WIMPs, collide with a mirror equipped with interferometers, the motion of a pendulum and the elastic oscillation of the mirror are excited. We performed a mode-analysis of possible signals caused by a WIMP collision with the mirror, and calculated the signal to noise ratio considering the design sensitivities of the existing or planned detectors and the “Thin-ET” detector. We derived that the signal to noise ratio may be  $1.7 \left( \frac{m_{\text{DM}}}{100 \text{ GeV}} \right)$  for the “Thin-ET” detector, we then estimated the upper limit on the cross section between a WIMP and a nucleon. Such an “Thin-ET” detector enables us to set more strict upper limits on the cross section in the low WIMP mass region ( $\lesssim 0.2 \text{ GeV}$ ) that has never been explored before. The limit would be improved by an order of

magnitude around  $m_{\text{DM}} = 0.2$  GeV.

- 
- [1] B. P. Abbott *et al.*, (LIGO Scientific Collaboration and Virgo Collaboration), Phys. Rev. Lett. **116**, 061102 (2016).
  - [2] B. P. Abbott *et al.*, (LIGO Scientific Collaboration and Virgo Collaboration), Phys. Rev. Lett. **116**, 241103 (2016).
  - [3] B. P. Abbott *et al.*, (LIGO Scientific Collaboration and Virgo Collaboration), Phys. Rev. Lett. **118**, 221101 (2017); Erratum Phys. Rev. Lett. **121**, 129901 (2018).
  - [4] B. P. Abbott *et al.*, (LIGO Scientific Collaboration and Virgo Collaboration), Phys. Rev. Lett. **119**, 141101 (2017).
  - [5] B. P. Abbott *et al.*, (LIGO Scientific Collaboration and Virgo Collaboration), Astroph. J. Lett. **851**, L25 (2017).
  - [6] B. P. Abbott *et al.*, (LIGO Scientific Collaboration and Virgo Collaboration), arXiv:1811.12907 [astro-ph.HE] (2018).
  - [7] B. P. Abbott *et al.*, (LIGO Scientific Collaboration and Virgo Collaboration), Phys. Rev. Lett. **119**, 161101 (2017).
  - [8] T. Akutsu *et al.*, (KAGRA Collaboration), Prog. Theor. Exp. Phys. **2018**, 013F01 (2018).
  - [9] T. Akutsu *et al.*, (KAGRA Collaboration), Class. Quant. Grav. **36**, 165008 (2019).
  - [10] T. Akutsu *et al.*, (KAGRA Collaboration), Nature Astronomy **3**, 35-40 (2019).
  - [11] K. Akiyama *et al.*, (KAGRA Collaboration), Class. Quant. Grav. **36**, 095015 (2019).
  - [12] M. Punturo *et al.*, Class. Quant. Grav. **27**, 194002 (2010).
  - [13] B. P. Abbott *et al.*, (LIGO Scientific Collaboration and Virgo Collaboration), Class. Quant. Grav. **34**, 044001 (2017).
  - [14] G. B. Gelmini, arXiv:hep-ph/1502.01320 (2015).
  - [15] X. J. Bi, P. F. Yui, and Q. Yuan, arXiv:1409.4590 [hep-ph] (2014).
  - [16] R. Bernabei *et al.*, (DAMA) Euro. Phys. J. **C56**, 333 (2008).
  - [17] R. Agnese *et al.*, (SuperCDMS Collaboration), Phys. Rev. Lett. **112**, 241302 (2014).
  - [18] C. E. Aalseth *et al.*, (CoGeNT Collaboration) Phys. Rev. D **88**, 012002 (2013).
  - [19] A. Kashlinsky, Astroph. J. Lett. **823**, L25 (2016).
  - [20] A. Aoki, J. Soda, Int. J. Mod. Phys. **D26**, 1750063 (2017).
  - [21] K. Yamamoto *et al.*, Phys. Rev. D **78**, 022004 (2008).
  - [22] L. Baudis, Physics of the Dark Universe **1**, 94 (2012).
  - [23] SRIM (The Stopping and Range of Ions in Matter), <http://www.srim.org>.
  - [24] J. D. E. Creighton and W. G. Anderson, *Gravitational-Wave Physics and Astronomy: An Introduction to Theory, Experiment and Data Analysis (Wiley Series in Cosmology)* (2011).
  - [25] LIGO Document, LIGO DCC T1500293-v11, <https://dcc.ligo.org/LIGO-T1500293-v11/public>.
  - [26] KAGRA Document, jgw-t1707038, [https://gwdoc.icrr.u-tokyo.ac.jp/DocDB/0070/T1707038/007/spectrum\\_DRSE.txt](https://gwdoc.icrr.u-tokyo.ac.jp/DocDB/0070/T1707038/007/spectrum_DRSE.txt).
  - [27] A. H. Abdelhameed *et al.*, (CRESST Collaboration), arXiv:1904.00498 [astro-ph.CO] (2019).
  - [28] G. Angloher *et al.*, (CRESST Collaboration), Euro. Phys. J. **C76**, 1 (2016).
  - [29] G. Angloher *et al.*, (CRESST Collaboration), Euro. Phys. J. **C77**, 637 (2017).
  - [30] Q. Yue *et al.*, (CDEX Collaboration), Phys. Rev. D **90**, 091701 (2014).
  - [31] R. Agnese *et al.*, (SuperCDMS Collaboration) Phys. Rev. Lett. **116**, 071301 (2016).
  - [32] A. Aguilar-Arevalo *et al.*, (DAMIC Collaboration) Phys. Rev. D **94**, 082006 (2016).
  - [33] L. Hehn *et al.*, Euro. Phys. J. **C76**, 548 (2016).
  - [34] E. Armengaud *et al.*, (EDELWEISS Collaboration), Phys. Rev. D **99**, 082003 (2019).
  - [35] R. Agnese *et al.*, (SuperCDMS Collaboration), Phys. Rev. Lett. **112**, 241302 (2014).
  - [36] C. E. Aalseth *et al.*, (CoGeNT Collaboration), Phys. Rev. D **88**, 012002 (2013).
  - [37] P. Agnes *et al.*, (DarkSide Collaboration), Phys. Rev. Lett. **121**, 081307 (2018).
  - [38] D. S. Akerib *et al.*, (LUX Collaboration), Phys. Rev. Lett. **118**, 021303 (2017).
  - [39] D. S. Akerib *et al.*, (LUX Collaboration), Phys. Rev. Lett. **122**, 131301 (2019).
  - [40] X. Cui *et al.*, (PandaX-II Collaboration), Phys. Rev. Lett. **119**, 181302 (2017).
  - [41] E. Aprile *et al.*, (XENON Collaboration), Phys. Rev. D **94**, 092001 (2016).
  - [42] E. Aprile *et al.*, (XENON Collaboration), Phys. Rev. Lett. **121**, 111302 (2018).
  - [43] G. Adhikari *et al.*, (The COSINE-100 Collaboration), Nature **564**, 83 (2018).
  - [44] J. I. Collar, Phys. Rev. D **98**, 023005 (2018).
  - [45] Q. Arnaud *et al.*, Astropart. Phys. **97**, 54 (2018).
  - [46] C. Amole *et al.*, (PICO Collaboration), Phys. Rev. D **93**, 052014 (2016).
  - [47] A. G tlein *et al.*, Astropart. Phys. **69**, 44 (2015).